Journal of Spatial Information Sciences

...JSIS

ASSESSMENT OF FLOOD VULNERABILITY ZONES IN ESAN SOUTH EAST LGA, EDO STATE, NIGERIA

OKEKE, U. C., EKEMEZIE, E. J

JOURNAL OF SPATIAL INFORMATION SCIENCES ISSN: 2354-3361
VOL. 3, ISSUE 1, PP 163–188, 2026 DOI: https://doi.org/10.5281/zenodo.20708638
PUBLISHED 15-05-2026

www.journals.unizik.edu.ng/jsis

ASSESSMENT OF FLOOD VULNERABILITY ZONES IN ESAN SOUTH EAST LGA, EDO STATE, NIGERIA

[1]Okeke, U. C., [2]Ekemezie, E. J.

[1,2]Department of Surveying and Geoinformatics, Nnamdi Azikiwe University Awka, Anambra State, Nigeria
[1]Corresponding Author: uc.okeke@unizik.edu.ng

DOI: https://doi.org/10.5281/zenodo.20708638

Abstract

Flooding remains a major environmental hazard that threatens lives, property, infrastructure, and agricultural activities in many parts of Nigeria. Effective flood risk management requires the identification and mapping of areas that are susceptible to flooding in order to support planning and mitigation efforts. This study assessed flood vulnerability zones in Esan South East Local Government Area, Edo State, Nigeria, using geospatial techniques and multi-criteria decision analysis. The specific objectives were to delineate the spatial distribution of flood-influencing factors, standardize the factors using fuzzy membership functions, determine factor weights through Principal Component Analysis (PCA), and generate a flood vulnerability map using the Weighted Linear Combination (WLC) approach. Five flood-conditioning factors comprising elevation, slope, proximity to drainage networks, proximity to water bodies, and watershed characteristics were derived from geospatial datasets. The factors were standardized using fuzzy membership functions and weighted using PCA before integration through WLC. The resulting flood vulnerability map was classified into Very Low, Low, Moderate, High, and Very High Vulnerability categories. The results showed that proximity to water bodies (22.27%) exerted the greatest influence on flood vulnerability, followed by elevation (20.28%), proximity to drainage networks (20.23%), slope (20.05%), and watershed characteristics (17.17%). The flood vulnerability assessment revealed that 30.69%, 27.22%, 19.07%, 6.33%, and 16.68% of the study area fall within the Very Low, Low, Moderate, High, and Very High Vulnerability classes respectively. Settlement vulnerability analysis identified 49 settlements located within High and Very High Vulnerability zones, with communities such as Asaboro Quarters, Omo Quarters II, Willy Quarters, Udeze Quarters, Ifianyi, Udenka Quarters, Okperu Quarters, Nana Quarters, Emmanuel Quarters, Ekuale Quarters, Odiotor, and Erobobo among those most exposed to flood hazards. The concentration of vulnerable settlements within Emu, Oria, Illushi, and Ewohimii wards highlights the potential threat of flooding to human settlements and socio-economic activities. The study demonstrates the effectiveness of integrating GIS, fuzzy logic, PCA, and WLC techniques for flood vulnerability assessment and provides a scientific basis for flood risk management, land-use planning, and disaster preparedness within Esan South East Local Government Area.

Keywords: Flood Vulnerability, Geographic Information Systems (GIS), Fuzzy Membership, Principal Component Analysis, Weighted Linear Combination.

1. Introduction

Flooding is one of the most widespread and destructive natural hazards globally, affecting millions of people annually and causing substantial losses to lives, property, infrastructure, and economic activities. Increasing urbanization, population growth, climate variability, and changes in land-use patterns have intensified the frequency and magnitude of flood events in many regions of the world, making flood risk management a major environmental and developmental concern [1][2]. Historical disaster records indicate that floods account for a significant proportion of global natural disasters and continue to produce extensive socio-economic and environmental consequences, particularly in developing countries where preparedness and adaptive capacities are often limited [3].

Hydrological systems are inherently complex due to the interaction of climatic, topographic, geological, and anthropogenic factors that influence runoff generation, flow concentration, and water accumulation within drainage basins [4]. Extreme rainfall events, prolonged precipitation, river overflow, inadequate drainage infrastructure, and inappropriate land-use practices frequently contribute to flood occurrence. Rainfall-runoff relationships play a fundamental role in flood generation because intense precipitation can rapidly exceed infiltration capacities and channel conveyance limits, resulting in widespread inundation [5][6]. Recent studies have further demonstrated that changing precipitation regimes associated with climate variability and climate change are increasing the likelihood of extreme flood events across many regions of the world [2].

Floods produce a wide range of adverse impacts on communities and ecosystems. Beyond direct damage to buildings, transportation networks, and public infrastructure, flood events often disrupt economic activities, reduce agricultural productivity, contaminate water resources, and increase the vulnerability of affected populations [7]. Flood disasters also create significant challenges for emergency response and evacuation planning because the rapid onset of flooding can restrict movement and reduce accessibility to safe locations [8][9]. Consequently, the identification of flood-prone areas has become an important component of disaster risk reduction, sustainable development planning, and environmental management.

Flood vulnerability assessment provides a framework for identifying locations that are susceptible to flood impacts based on their physical, environmental, and socio-economic characteristics. Traditional flood assessment approaches often rely on hydrological and hydraulic modelling techniques; however, these methods frequently require extensive datasets, substantial computational resources, and detailed field measurements that may not be readily available in many developing regions [10]. Advances in Geographic Information Systems (GIS), remote sensing, and spatial decision-support techniques have provided alternative approaches for flood vulnerability assessment by enabling the integration of multiple flood-conditioning factors within a spatially explicit analytical environment [11][12].

GIS-based flood vulnerability mapping has gained considerable attention because of its ability to integrate diverse environmental variables, visualize spatial patterns, and support decision-making processes. Multi-Criteria Decision Analysis (MCDA) techniques are particularly useful in this regard because flooding is influenced by several interrelated factors rather than a single environmental variable. Factors such as elevation, slope, drainage characteristics, proximity to water bodies, and watershed conditions collectively determine the likelihood of flood occurrence and its spatial distribution [10][11]. The integration of these factors within a GIS environment enables the generation of flood vulnerability maps that can support planning, mitigation, and emergency preparedness efforts.

Recent studies have demonstrated the effectiveness of combining GIS with fuzzy logic and other multi-criteria approaches for flood risk and vulnerability assessment. Fuzzy logic techniques are particularly advantageous because they accommodate the inherent uncertainty and gradual transitions associated with environmental processes, thereby providing a more realistic representation of flood vulnerability [13]. Similarly, GIS-based multi-criteria frameworks have been successfully applied in different geographical settings to identify flood-prone areas, prioritize vulnerable zones, and support disaster management initiatives [7][10][11]. Such approaches have proven valuable for reducing uncertainty in spatial decision-making and improving the effectiveness of flood risk management strategies.

Despite increasing recognition of flood hazards in Nigeria, many local government areas continue to experience recurring flood events without adequate spatial information to guide mitigation and adaptation measures. The absence of detailed flood vulnerability maps limits the ability of planners and decision-makers to identify high-risk areas, prioritize interventions, and implement evidence-based flood management strategies. Esan South East Local Government Area of Edo State is not exempt from these challenges. Seasonal rainfall, expanding human activities, and the influence of natural drainage systems create conditions that may increase flood vulnerability in parts of the area. However, comprehensive geospatial assessments capable of identifying vulnerable locations and settlements at risk remain limited.

The application of geospatial techniques for flood vulnerability assessment in Esan South East LGA therefore provides an opportunity to generate scientifically based information for flood risk management and sustainable land-use planning. By integrating flood-conditioning factors within a GIS-based analytical framework, vulnerable areas can be identified and classified according to their vulnerability levels. Such information is important for supporting disaster preparedness, infrastructure development, environmental management, and community resilience initiatives.

This study therefore assessed flood vulnerability zones in Esan South East Local Government Area, Edo State, Nigeria, using geospatial techniques. The study integrated elevation, slope, proximity to drainage networks, proximity to water bodies, and watershed characteristics within a GIS environment to delineate flood vulnerability zones and identify settlements exposed to flood hazards. The findings are expected to provide valuable information for flood mitigation planning, disaster risk reduction, and sustainable development within the study area.

2. Materials and Methods

2.1. Study Area

Esan South East Local Government Area is located in the central senatorial district of Edo State, southern Nigeria. The Local Government Area lies approximately between latitudes 6°30′N and 6°50′N and longitudes 6°00′E and 6°30′E (Figure 1), covering a land area of about 1,302 km². Its administrative headquarters is located at Ubiaja, which serves as the major commercial and administrative centre of the area. Esan South East shares boundaries with Esan North East and

Esan Central Local Government Areas to the north, Iguegben Local Government Area to the west, and parts of Kogi and Delta States to the east and south respectively.

The area is characterized by a gently undulating terrain with elevations ranging from low-lying valley bottoms to moderately elevated uplands. Numerous streams and drainage channels traverse the landscape, forming interconnected watershed systems that influence surface runoff and flood occurrence. The climate is tropical, with distinct wet and dry seasons. Annual rainfall is generally high, occurring mainly between April and October, while temperatures remain relatively high throughout the year. These climatic conditions contribute significantly to runoff generation during periods of intense precipitation.

Vegetation within the area is predominantly derived savannah interspersed with agricultural lands, settlements, and patches of secondary forest. Agriculture constitutes a major economic activity, with residents engaged in the cultivation of crops such as cassava, yam, maize, and oil palm. The presence of extensive agricultural land, growing settlements, and drainage networks makes the area susceptible to flood-related impacts, particularly during periods of heavy rainfall. These environmental and socio-economic characteristics make Esan South East Local Government Area suitable for flood vulnerability assessment using geospatial techniques.

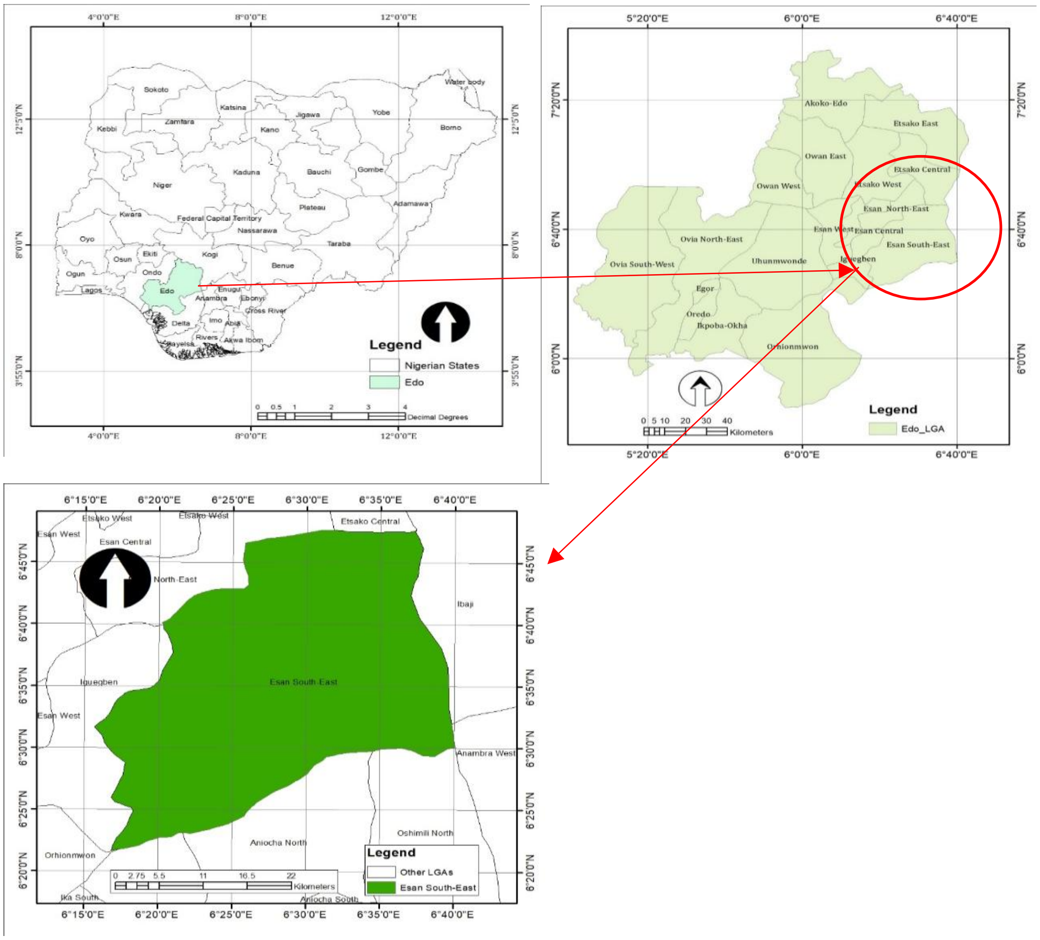

Figure 1: Map of the Study Area

2.2. Methodology

The study adopted a GIS-based multi-criteria decision analysis approach for assessing flood vulnerability in Esan South East Local Government Area, Edo State. Spatial datasets comprising Digital Elevation Model (DEM), drainage networks, water bodies, and administrative boundary data were acquired and processed within the ArcGIS Pro environment. The datasets were projected to a common coordinate system and clipped to the boundary of the study area to ensure spatial consistency during analysis.

2.2.1. Identification of Flood Risk Factors

Five flood-driving factors were considered based on their influence on flood generation and propagation:

1. Elevation
2. Slope
3. Proximity to Waterbodies
4. Proximity to Drainage Networks
5. Watershed Characteristics

Elevation was extracted directly from the SRTM DEM. Areas with lower elevations were considered more susceptible to flooding because they act as natural zones for runoff accumulation and water stagnation. Slope was derived from the DEM using the Spatial Analyst Slope function. Slope was calculated using equation 1:

$$S = \tan^{-1}\left(\sqrt{\left(\frac{dz}{dx}\right)^2 + \left(\frac{dz}{dy}\right)^2}\right) \qquad \dots(1)$$

where:
(S) = slope angle,
$\left(\frac{dz}{dx}\right)$ = rate of elevation change in the x-direction,
$\left(\frac{dz}{dy}\right)$ = rate of elevation change in the y-direction.

Lower slope values were considered more favourable for flood occurrence because of reduced runoff velocity.

The Euclidean Distance tool was used to calculate the distance of each raster cell from the nearest drainage channel. Areas located closer to drainage networks were considered more susceptible to flooding because of their exposure to channel overflow during heavy rainfall events.

The Euclidean distance was calculated as in equation 2:

$$D = \sqrt{(x_2 - x_1)^2 + (y_2 - y_1)^2} \qquad \dots(2)$$

where:

(D) = Euclidean distance,
(x_1, y_1) = coordinates of the source feature,
(x_2, y_2) = coordinates of the target location.

Distance to water bodies was similarly generated using the Euclidean Distance function. Areas closer to rivers and streams were assumed to possess higher flood vulnerability due to the likelihood of river overflow and floodplain inundation. Watershed boundaries were delineated from the DEM using hydrological analysis tools. The process involved sink filling, flow direction generation, flow accumulation analysis, and watershed delineation. Flow direction was computed using the D8 algorithm, where runoff from each raster cell is assigned to the steepest downslope neighbour.

The flow accumulation value for each cell was determined as in equation 3:

$$FA_i = \sum_{j=1}^{n} W_j \qquad \dots (3)$$

where:

(FA_i) = flow accumulation at cell (i),
$\left(W_j\right)$ = contributing upstream cells,
(n) = total number of upstream cells draining into cell (i).

Higher watershed influence values indicate greater runoff convergence and increased flood vulnerability.

2.2.2. Fuzzy Membership Standardization

The extracted factors were measured in different units and scales, making direct integration unsuitable. Consequently, fuzzy membership functions were employed to standardize all criteria to a common scale ranging from 0 to 1. The Fuzzy Small membership function was applied to elevation, slope, proximity to drainage networks, and proximity to water bodies because lower values correspond to higher flood vulnerability. Conversely, the Fuzzy Large membership function was applied to watershed characteristics because larger watershed influence values increase flood potential.

The general fuzzy membership function is expressed as in equation 4:

$$\mu(x) = \frac{1}{1 + \left(\frac{x}{f}\right)^{s}} \qquad \dots (4)$$

where:

$\left(\mu(x)\right)$ = membership value,
(x) = input variable,
(f) = midpoint parameter,
(s) = spread parameter.

Membership values approaching 1 indicate greater flood vulnerability, while values approaching 0 indicate lower vulnerability.

2.2.3. Principal Component Analysis (PCA) Weighting

Principal Component Analysis (PCA) was employed to objectively determine the relative importance of the flood-conditioning factors. PCA reduces data redundancy by transforming correlated variables into a set of uncorrelated principal components. The data were standardized using equation 5:

$$Z_i = \frac{X_i - \mu}{\sigma} \qquad \dots(5)$$

where:

(Z_i) = standardized value,
(X_i) = original value,
(μ) = mean,
(σ) = standard deviation.

The covariance matrix was then generated and decomposed into eigenvalues and eigenvectors according to equation 6:

$$|C - \lambda I| = 0 \qquad \dots(6)$$

where:

(C) = covariance matrix,
(λ) = eigenvalue,
(I) = identity matrix.

The percentage variance explained by each component was calculated as in equation 7:

$$PV_i = \frac{\lambda_i}{\sum \lambda_i} \times 100 \qquad \dots(7)$$

where:
(PV_i) = percentage variance explained by component (i),

(λ_i) = eigenvalue of component (i).

The final PCA weights were obtained by normalizing the contribution of each factor with equation 8:

$$W_i = \frac{L_i}{\sum L_i} \qquad \dots(8)$$

where:

(W_i) = weight of factor (i),

(L_i)= loading score of factor (i).

2.2.4. Flood Vulnerability Modelling Using Weighted Linear Combination

The standardized factors and PCA-derived weights were integrated using the Weighted Linear Combination (WLC) technique to generate the flood vulnerability index.

The WLC model is expressed as equation 9:

$$FVI = \sum_{i=1}^{n} (W_i \times X_i) \qquad \ldots (9)$$

where:

(FVI) = Flood Vulnerability Index,

(W_i) = weight assigned to factor (i),

(X_i) = fuzzy standardized factor value,

(n) = number of factors.

For this study:

$$FVI = (0.2227 \times PWB) + (0.2028 \times ELEV) + (0.2023 \times PDN) + (0.2005 \times SLOPE) + (0.1717 \times WAT)$$

where:
PWB = Proximity to Water Bodies,
ELEV = Elevation,
PDN = Proximity to Drainage Networks,
SLOPE = Slope,
WAT = Watershed Characteristics.

The resulting flood vulnerability index was classified into five categories using the Natural Breaks (Jenks) classification method:

1. Very Low Vulnerability
2. Low Vulnerability
3. Moderate Vulnerability
4. High Vulnerability
5. Very High Vulnerability

2.2.5. Identification of Settlements at Risk

The final flood vulnerability map was overlaid with the settlement layer using spatial overlay analysis. Settlement locations intersecting the High and Very High Vulnerability zones were extracted and identified as settlements at risk. The analysis enabled the determination of communities potentially exposed to flood hazards and provided spatial information for disaster preparedness and flood risk management within the study area.

3. Results

3.1. Spatial Distribution of Flood Influencing Criteria in Esan South East Local Government Area

The spatial distribution of the factors influencing flood vulnerability in Esan South East Local Government Area, Edo State, was examined using elevation, watershed characteristics, proximity to water bodies, proximity to drainage networks, and slope. These factors were selected because of their influence on surface runoff generation, flow concentration, drainage behaviour, and water accumulation within the landscape. Understanding their spatial patterns provides insight into areas that are naturally predisposed to flooding and forms the basis for subsequent flood vulnerability assessment. The spatial distribution of these flood-influencing criteria is presented in Figure 2.

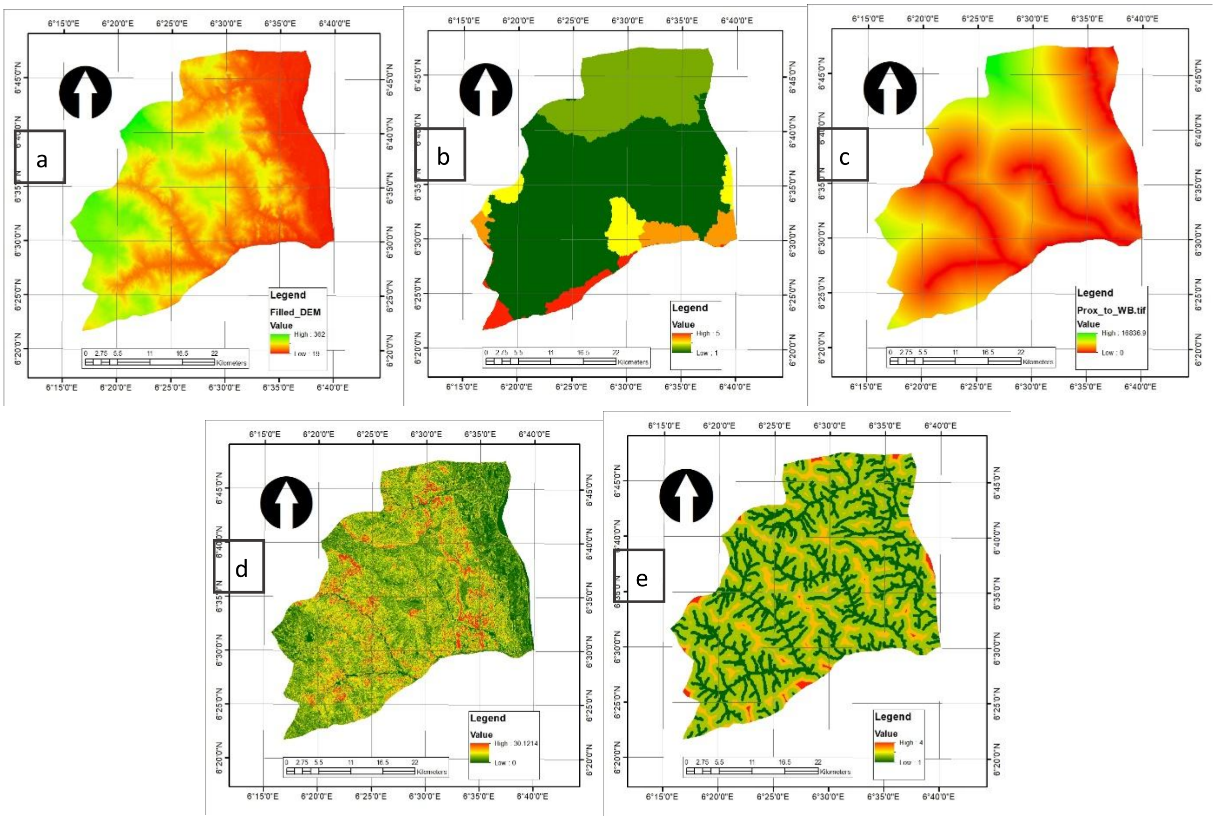

Figure 2: Spatial Distribution of (a) Elevation, (b) Watershed, (c) Proximity to Waterbody, (d) Slope, and (e) Proximity to Drainage Network in Esan South-East Local Government Area, Edo State

The elevation map of Esan South East LGA (Figure 2a) reveals considerable topographic variation across the study area, with elevation values ranging from approximately 19 m to 362 m above mean sea level. Areas represented by green colours correspond to higher elevations, while orange and red colours indicate lower terrain.. This spatial configuration suggests that runoff generated from the elevated eastern and northeastern uplands is naturally directed towards the lower central and western portions of the LGA. The hydrological implication of this pattern is that low-lying areas are more susceptible to water accumulation, prolonged inundation, and flood occurrence because they function as natural receiving zones for runoff originating from higher elevations. Conversely, elevated areas facilitate runoff generation and generally experience lower flood vulnerability due to improved drainage conditions.

The watershed map (Figure 2b) illustrates the hydrological catchment structure of the study area. Four watershed classes were identified, representing varying levels of runoff concentration and drainage convergence. The map reveals a well-developed dendritic drainage pattern distributed throughout the LGA. Numerous drainage tributaries converge into larger channels, creating interconnected watershed systems. Areas characterized by higher watershed values are concentrated along major drainage corridors and stream confluences, where runoff from extensive upstream catchments accumulates. The distribution indicates that substantial portions of the LGA contribute runoff to a network of interconnected drainage basins. Locations situated within major watershed outlets are likely to receive large volumes of surface flow during intense rainfall events, increasing their vulnerability to flooding. Areas positioned along watershed convergence zones are therefore expected to experience greater flood vulnerability than locations situated on watershed divides.

The proximity-to-water-body map (Figure 2c) shows distances ranging from 0 m to approximately 16,836.9 m from major water bodies within the study area. Areas represented by red colours are located closest to rivers, streams, and other surface water features, while green-coloured areas are situated farther away. The spatial pattern indicates that major drainage corridors traverse the central, southern, and eastern portions of the LGA, creating extensive zones of close proximity to water bodies.

Locations adjacent to rivers and streams exhibit increased flood vulnerability because they are exposed to channel overflow during periods of intense rainfall. Floodwaters can easily spill beyond channel banks, inundating nearby settlements and agricultural lands. As distance from water bodies increases, flood vulnerability generally decreases due to reduced exposure to riverine flooding processes. The proximity analysis therefore identifies river corridors and adjacent floodplains as the most vulnerable locations within the study area.

The slope map (Figure 2d) indicates significant spatial variation in terrain steepness across Esan South East LGA, with slope values ranging from approximately 0° to 30.12°. Areas characterized by low slopes are represented by green colours, while red colours indicate steeper terrain. Gentle slopes dominate much of the study area, particularly within the central and eastern sections, whereas steep slopes occur mainly along dissected valleys and drainage channels. Slope exerts a direct influence on runoff velocity and infiltration processes. Areas with very gentle slopes promote reduced flow velocity, increased water retention, and ponding conditions, thereby increasing flood vulnerability.

Conversely, steeper slopes facilitate rapid runoff movement and reduce the duration of water accumulation. The predominance of low to moderate slopes across large portions of the LGA suggests favourable conditions for runoff concentration and temporary water storage, particularly where gentle slopes coincide with low elevations and proximity to drainage channels.

The drainage network proximity map (Figure 2e) classifies the study area into five proximity zones relative to major drainage channels. The spatial distribution reveals that extensive portions of the LGA are located close to drainage networks, particularly within the central and southern sectors. Areas represented by red and orange colours are situated nearest to drainage channels and therefore possess the highest flood vulnerability. Yellow-coloured areas represent moderate proximity, while green-coloured zones are located farther from drainage networks and are relatively less vulnerable. The concentration of high-proximity zones along drainage corridors indicates that flooding is likely to occur first within these areas during periods of heavy rainfall. Overflow from channels, combined with runoff accumulation from surrounding catchments, may result in localized inundation. The extensive coverage of moderate-to-high proximity classes suggests that a substantial proportion of the LGA is hydrologically connected to the drainage system and therefore potentially exposed to flood hazards.

The combined analysis of the flood-influencing criteria reveals distinct spatial variations in flood vulnerability across Esan South East LGA. Low-elevation areas, gentle slopes, watershed convergence zones, and locations situated close to rivers and drainage channels exhibit the greatest potential for flood occurrence. These conditions are particularly evident within the central, southwestern, and southern portions of the LGA, where multiple flood-promoting factors coincide.
Higher elevations observed along the eastern and northeastern sectors facilitate runoff generation, which is subsequently transported downslope towards lower terrain. The extensive drainage network and interconnected watershed systems further enhance runoff concentration within valley bottoms and floodplain environments. The spatial relationships among these factors indicate that flood vulnerability within Esan South East LGA is controlled by the interaction between topography, hydrological connectivity, and proximity to surface water systems. The delineation of these criteria therefore provides the foundation for subsequent standardization, weighting, and flood vulnerability modelling.

3.2. Reclassification and Standardization of Flood Vulnerability Factors Using Fuzzy Membership Functions

Following the analysis of the spatial distribution of the flood-conditioning factors, all criteria were standardized using fuzzy membership functions to transform the datasets into a common scale ranging from 0 to 1. This standardization process was necessary because the factors were measured in different units and possessed varying numerical ranges. Fuzzy membership functions provide a gradual representation of flood vulnerability by assigning each location a degree of membership

ISSN: 2354-3361
DOI: https://doi.org/10.5281/zenodo.20708638
www.journals.unizik.edu.ng/jsis

based on its contribution to flood occurrence. Membership values approaching 1 indicate higher vulnerability to flooding, whereas values closer to 0 represent lower vulnerability. The fuzzy standardization scheme adopted for the study is presented in Table 1, while the resulting fuzzy membership maps are shown in Figure 3.

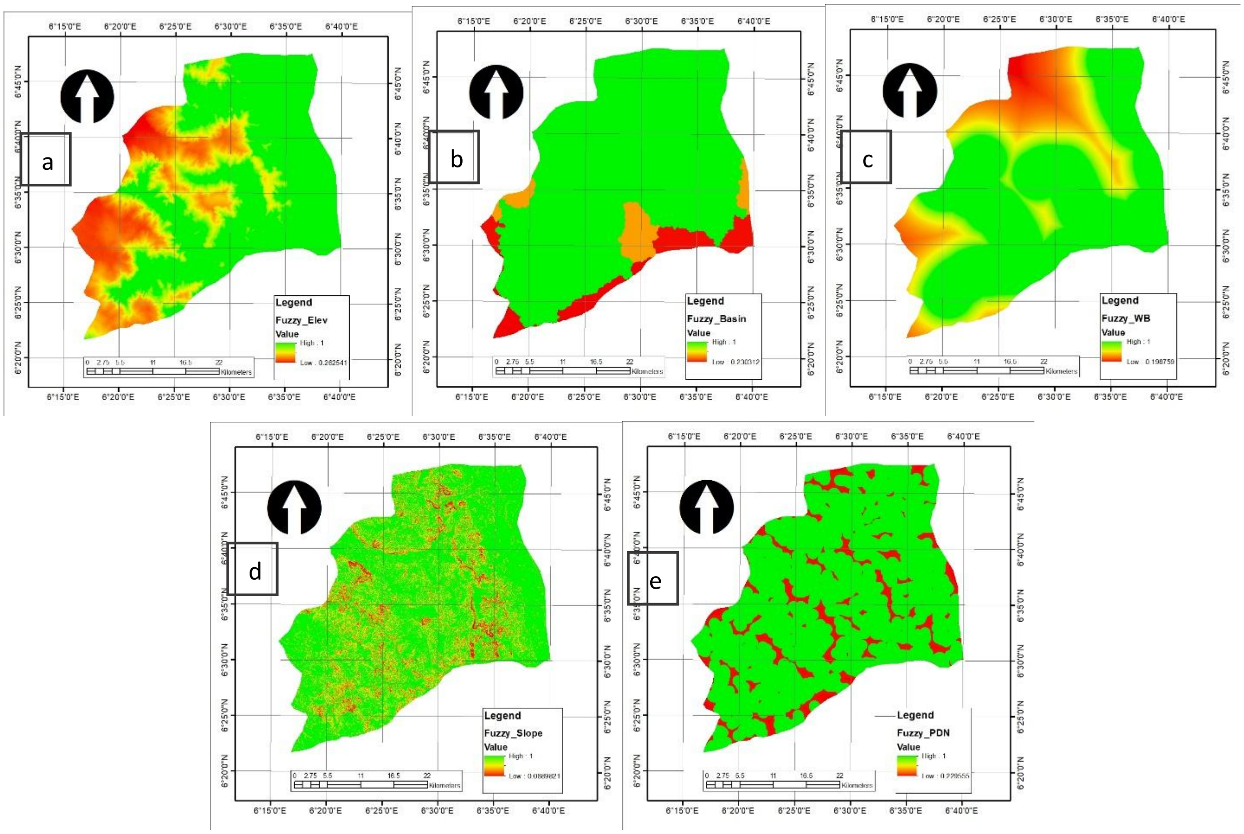

Figure 3: Reclassification and Standardization of (a) Elevation, (b) Watershed, (c) Proximity to Waterbody, (d) Slope, and (e) Proximity to Drainage Network in Esan South-East Local Government Area, Edo State

Table 1: Fuzzy Membership Standardization Scheme for Flood Vulnerability Factors

Factor	Fuzzy Function	Input Range	Membership Range	Flood Influence
Elevation	Fuzzy Small	19–362 m	0.263–1.000	Lower elevations assigned higher membership values
Slope	Fuzzy Small	0–30.12°	0.089–1.000	Gentle slopes assigned higher membership values
Proximity to Drainage Network	Fuzzy Small	0–4 km	0.230–1.000	Areas closer to drainage assigned higher membership values

Proximity to Water Bodies	Fuzzy Small	0–16,836.9 m	0.199–1.000	Areas nearer water bodies assigned higher membership values
Watershed Characteristics	Fuzzy Large	Watershed Classes 1–5	0.230–1.000	Higher watershed influence assigned higher membership values

Table 1 illustrates that the Fuzzy Small membership function was applied to elevation, slope, proximity to drainage networks, and proximity to water bodies because lower values of these variables are generally associated with higher flood vulnerability. In contrast, the watershed criterion was standardized using the Fuzzy Large function since higher watershed influence corresponds to increased runoff concentration and flood potential.

The fuzzy standardized elevation layer (Figure 3a) generated membership values ranging from 0.263 to 1.000, as indicated in Table 1. The application of the Fuzzy Small function assigned higher membership values to lower elevations and progressively reduced membership values with increasing elevation.

The spatial pattern reveals that high membership values are concentrated within the eastern and southeastern portions of the study area, indicating zones that are more susceptible to runoff accumulation and flood inundation. Moderate membership values occur within the central section, while lower membership values are observed within elevated areas of the western and southwestern regions.

The results demonstrate the significant influence of topography on flood occurrence. Lower terrain functions as natural runoff receiving zones where water accumulates during rainfall events, thereby increasing flood vulnerability. The elevation standardization therefore effectively identifies low-lying landscapes with greater flood vulnerability.

The fuzzy slope layer (Figure 3b) produced membership values ranging from 0.089 to 1.000, using the Fuzzy Small membership function, gentle slopes received higher membership values, whereas steeper slopes were assigned lower values. The standardized map indicates that a substantial proportion of Esan South East LGA is characterized by high membership values. Green-coloured areas dominate the landscape, suggesting the prevalence of gentle terrain conditions across much of the LGA. Lower membership values are confined mainly to dissected valleys and localized steep terrain. The predominance of high fuzzy values reflects favourable conditions for surface water accumulation because gentle slopes reduce runoff velocity and increase the likelihood of ponding. Consequently, slope contributes significantly to flood vulnerability within the study area. The widespread distribution of high-membership zones indicates that topographic gradients are generally conducive to flood development.

The fuzzy proximity-to-drainage-network layer (Figure 3c) generated membership values ranging from 0.230 to 1.000. The Fuzzy Small function assigned the highest membership values to locations closest to drainage channels and progressively lower values with increasing distance. The resulting map reveals numerous high-membership zones distributed throughout the study area, reflecting the extensive drainage network identified during the spatial analysis stage. Areas immediately adjacent to drainage channels exhibit the highest vulnerability values because they are more likely to experience channel overflow and concentrated runoff during periods of intense rainfall. The extensive occurrence of high fuzzy values demonstrates that a considerable proportion of the LGA is hydrologically connected to drainage systems. This condition increases exposure to flooding and emphasizes the significance of drainage proximity as a controlling factor in flood vulnerability assessment.

The fuzzy proximity-to-water-body layer (Figure 3d) produced membership values ranging from 0.199 to 1.000. The Fuzzy Small membership function assigned higher vulnerability values to areas located near rivers, streams, and other water bodies. The standardized map indicates that the highest membership values occur along major river corridors and drainage systems, particularly within the northern, western, and southwestern sections of the study area. Membership values gradually decrease with increasing distance from water bodies. This spatial pattern reflects the direct relationship between flood occurrence and proximity to hydrological features. Areas situated close to rivers and streams are exposed to river overflow, backwater effects, and floodplain inundation, making them more susceptible to flooding. The fuzzy standardization therefore effectively captures the spatial influence of water bodies on flood vulnerability.

The fuzzy watershed layer (Figure 3e) generated membership values ranging from 0.230 to 1.000. Unlike the other factors, watershed characteristics were standardized using the Fuzzy Large function because areas with greater watershed influence contribute more significantly to runoff concentration and flow accumulation. The map reveals extensive areas of high membership values across the northern, central, and eastern sectors of the LGA. Lower membership values are largely confined to portions of the southern boundary and isolated peripheral locations. The dominance of high fuzzy values indicates that large sections of Esan South East LGA are located within catchment areas that receive runoff from extensive upstream drainage systems. These locations are more susceptible to flooding because of increased flow convergence and runoff accumulation. The watershed criterion therefore represents an important hydrological control on flood vulnerability within the study area.

3.3. Principal Component Analysis (PCA) Weighting of Flood Vulnerability Factors

Following the fuzzy standardization of the flood-conditioning factors, Principal Component Analysis (PCA) was applied to determine the relative contribution of each factor to flood vulnerability within Esan South East Local Government Area. PCA is a multivariate statistical technique that reduces data dimensionality by transforming correlated variables into a smaller number of uncorrelated principal components while preserving most of the variability contained in the original datasets. Prior to PCA computation, all standardized factors were subjected to correlation analysis to evaluate the degree of interrelationship among the variables. The resulting correlation matrix is presented in Table 2.

Table 2: Correlation Matrix of Flood Vulnerability Factors

Factor	Elevation	Slope	Proximity to Drainage Network	Proximity to Water Bodies	Watershed
Elevation	1.000	0.094	0.224	0.337	-0.128
Slope	0.094	1.000	0.084	0.017	-0.039
Proximity to Drainage Network	0.224	0.084	1.000	0.060	0.096
Proximity to Water Bodies	0.337	0.017	0.060	1.000	0.149
Watershed	-0.128	-0.039	0.096	0.149	1.000

Table 2 indicates generally weak to moderate correlations among the flood-conditioning factors, suggesting that each variable contributes unique information to the flood vulnerability model. The strongest positive correlation was observed between elevation and proximity to water bodies ($r = 0.337$), while watershed characteristics exhibited weak negative relationships with elevation ($r = -0.128$) and slope ($r = -0.039$). The absence of strong multicollinearity confirms the suitability of the dataset for PCA application. The eigenvalues and percentage variance explained by each principal component are presented in Table 3.

Table 3: Eigenvalues and Variance Explained by Principal Components

Principal Component	Eigenvalue	Variance Explained (%)	Cumulative Variance (%)
PC1	1.4626	29.25	29.25
PC2	1.1175	22.35	51.60
PC3	0.9997	19.99	71.59
PC4	0.8957	17.91	89.50
PC5	0.5244	10.49	100.00

The results presented in Table 3 show that the first principal component (PC1) accounts for 29.25% of the total variance within the dataset, making it the most influential component. The second principal component contributes an additional 22.35%, resulting in a cumulative variance of 51.60%. The first three principal components collectively explain 71.59% of the total variance, indicating that most of the information contained in the original variables is captured by these components. The cumulative variance reaches 89.50% after the fourth component and 100% after the fifth component. The PCA-derived weights calculated from the component loadings and variance contributions are presented in Table 4.5.

Table 4: PCA-Derived Weights for Flood Vulnerability Factors

Factor	PCA Weight	Weight (%)	Rank
Proximity to Water Bodies	0.2227	22.27	1
Elevation	0.2028	20.28	2
Proximity to Drainage Network	0.2023	20.23	3
Slope	0.2005	20.05	4
Watershed Characteristics	0.1717	17.17	5
Total	1.0000	100.00	—

Table 4. reveals that proximity to water bodies received the highest weight (22.27%), indicating that distance from rivers and streams exerts the greatest influence on flood vulnerability within Esan South East LGA. This finding reflects the direct role of river overflow, floodplain inundation, and channel expansion during intense rainfall events. Areas located close to water bodies are therefore more susceptible to flooding than locations situated farther away.

Elevation was assigned the second highest weight (20.28%), highlighting the importance of topographic controls on flood occurrence. Low-lying areas naturally function as runoff accumulation zones and consequently experience greater flood vulnerability. Proximity to drainage networks ranked third with a weight of 20.23%, demonstrating the significance of drainage density and channel connectivity in controlling surface water movement and concentration.

Slope contributed 20.05% to the overall model, indicating that terrain gradient exerts a substantial influence on runoff velocity and water retention. Gentle slopes favour water accumulation and prolonged inundation, whereas steeper slopes facilitate rapid runoff evacuation. Watershed characteristics received the lowest weight (17.17%), although the factor remains important because watershed configuration controls runoff convergence and catchment-scale hydrological behaviour.

The relatively balanced distribution of weights among the five factors suggests that flood vulnerability in Esan South East LGA is governed by the combined interaction of topographic and hydrological processes rather than by a single dominant factor. Nevertheless, the higher weights assigned to proximity to water bodies, elevation, and drainage proximity indicate that hydrological connectivity and terrain configuration constitute the primary controls on flood occurrence within the study area.

The PCA-derived weights presented in Table 4 were subsequently employed in the weighted overlay analysis to generate the final flood vulnerability map of Esan South East Local Government Area.

3.4 **Integration of Flood Vulnerability Factors Using Weighted Linear Combination (WLC)**

Following the fuzzy standardization and PCA weighting of the flood-conditioning factors, the Weighted Linear Combination (WLC) technique was employed to integrate the standardized criteria and produce the final flood vulnerability map of Esan South East Local Government Area. The WLC method combines the standardized factor layers according to their relative importance, thereby generating a composite flood vulnerability index for each raster cell within the study area. The PCA-derived weights used in the integration process are presented in Table 5.

Table 5: PCA-Derived Weights Used in Weighted Linear Combination

Factor	Weight
Proximity to Water Bodies	0.2227
Elevation	0.2028
Proximity to Drainage Network	0.2023
Slope	0.2005
Watershed Characteristics	0.1717
Total	1.0000

The flood vulnerability index (FVI) was computed using Equation 1:

$$\begin{aligned} FVI = {} & (0.2227 \times PWB) + (0.2028 \times ELEV) + (0.2023 \times PDN) + (0.2005 \times SLOPE) \\ & + (0.1717 \times WAT) FVI \\ & = (0.2227 \times PWB) + (0.2028 \times ELEV) + (0.2023 \times PDN) \\ & + (0.2005 \times SLOPE) + (0.1717 \times WAT) FVI \\ & = (0.2227 \times PWB) + (0.2028 \times ELEV) + (0.2023 \times PDN) \\ & + (0.2005 \times SLOPE) + (0.1717 \times WAT) \end{aligned}$$

Where:

FVI = Flood Vulnerability Index
PWB = Fuzzy standardized proximity to water bodies
ELEV = Fuzzy standardized elevation
PDN = Fuzzy standardized proximity to drainage network
SLOPE = Fuzzy standardized slope
WAT = Fuzzy standardized watershed characteristics

The weighted overlay operation produced a continuous flood vulnerability surface, which was subsequently classified into five vulnerability categories: Very Low, Low, Moderate, High, and Very High Vulnerability. The resulting flood vulnerability classes are presented in Figure 4, while their areal distribution is summarized in Table 6.

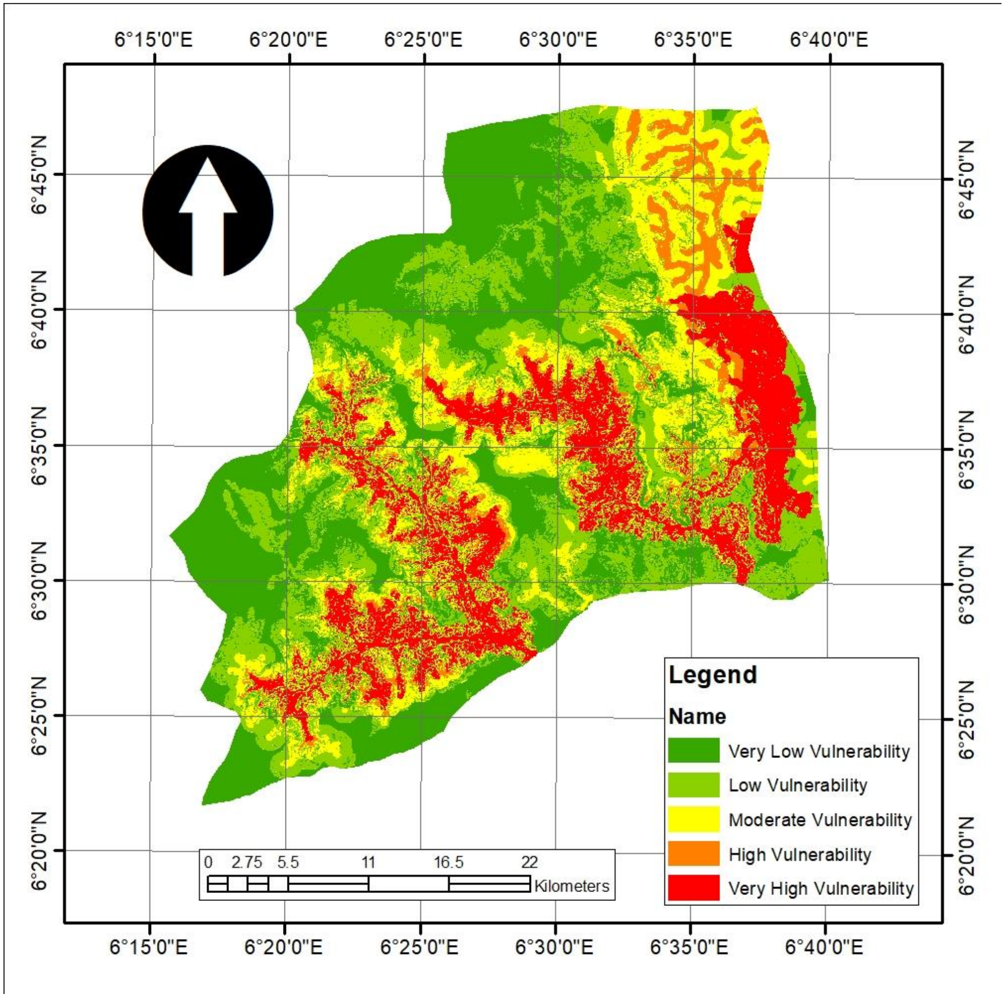

Figure 4: Flood Vulnerability Zones in Esan South-East LGA

Table 6: Spatial Distribution of Flood Vulnerability Zones in Esan South East LGA

Vulnerability Class	Area (km²)	Percentage (%)
Very Low Vulnerability	399.65	30.69
Low Vulnerability	354.48	27.22
Moderate Vulnerability	248.29	19.07
High Vulnerability	82.46	6.33
Very High Vulnerability	217.22	16.68
Total	1302.10	100.00

Table 6 shows that Very Low Vulnerability areas occupy the largest proportion of the study area, covering 399.65 km² (30.69%). These areas are predominantly located along the western, southwestern, and portions of the northern sectors of the LGA. Such locations are characterized by relatively favourable topographic and hydrological conditions, including greater distances from major water bodies and drainage channels, reduced runoff convergence, and lower vulnerability to flood accumulation.

Low Vulnerability areas account for 354.48 km² (27.22%) of the total land area. These zones occur extensively around the peripheral sections of the LGA and represent locations where flood-generating conditions are present but less pronounced. Together, the Very Low and Low Vulnerability categories constitute 57.91% of the study area, indicating that more than half of the LGA experiences relatively low vulnerability to flooding. Moderate Vulnerability areas cover 248.29 km², representing 19.07% of the total area. These zones form transitional regions between low-risk and high-risk environments and are distributed mainly around the central portions of the LGA. Flood occurrence within these locations is likely under conditions of prolonged or intense rainfall.

High Vulnerability zones occupy 82.46 km² (6.33%), representing the smallest vulnerability category. These areas occur primarily around major drainage corridors and zones of runoff concentration. Although spatially limited, these locations possess environmental conditions that favour frequent flooding. Very High Vulnerability areas cover 217.22 km², representing 16.68% of the study area. These zones are concentrated predominantly within the central, southeastern, eastern, and parts of the southern sections of the LGA. The spatial pattern observed in Figure 4.3 indicates that these areas coincide with locations characterized by low elevations, gentle slopes, close proximity to drainage systems and water bodies, and strong watershed influence. Such conditions promote runoff accumulation and significantly increase flood vulnerability. The results further reveal that High and Very High Vulnerability zones collectively account for 299.68 km² or 23.01% of the total land area. This indicates that nearly one-quarter of Esan South East LGA is exposed to considerable flood risk and may require priority attention in flood management and mitigation planning.

3.5 Settlements at Risk of Flooding in Esan South East LGA

To evaluate the potential impact of flooding on human settlements, the flood vulnerability map was overlaid with settlement locations within the study area. The analysis identified 205 settlements distributed across the five flood vulnerability classes. The distribution of settlements according to vulnerability level is presented in Table 7.

Table 7: Distribution of Settlements Across Flood Vulnerability Classes

Vulnerability Class	Number of Settlements	Percentage (%)
Very Low Vulnerability	47	22.93
Low Vulnerability	58	28.29
Moderate Vulnerability	51	24.88
High Vulnerability	18	8.78
Very High Vulnerability	31	15.12
Total	205	100.00

The results in Table 7 indicate that 49 settlements, representing 23.90% of all settlements within the LGA, are located within High and Very High Vulnerability zones. This finding demonstrates that a substantial proportion of the population is potentially exposed to recurrent flooding and its associated socio-economic impacts. The settlements identified within the Very High Vulnerability category are presented in Table 8.

Table 8: Settlements Located in Very High Flood Vulnerability Zones

Settlement	Ward
Asaboro Quarters	Ewohimii
Omo Quarters II	Ewohimii
Willy Quarters	Emu
Udeze Quarters	Emu
Ifianyi	Oria
Udenka Quarters	Oria
Anukuchubi Quarters	Oria
Adi Quarters	Oria
Amedu Quarters	Oria
Ugu	Emu
Isigue Quarters	Emu
Sunday Quarters II	Oria
Umuachala	Emu
Atomba Quarters	Emu
Ololo Quarters	Emu
Lawrence Quarters	Emu
Nneke Quarters I and II	Emu
Ifeanyi Quarters I	Emu
Nnabeyi Quarters	Emu
Gbogidi Quarters	Emu
Chibougo Quarters	Emu
Showboy Quarters	Emu
Mike Quarters	Oria
Okperu Quarters	Illushi
Nana Quarters	Illushi
Akpalaji Quarters	Illushi
Urhobo Quarters	Oria
Atamata Quarters	Oria
Ega Quarters II	Illushi
Alika Quarters	Illushi

Table 8 reveals a pronounced concentration of very highly vulnerable settlements within Emu, Oria, and Illushi wards. These settlements are situated close to major drainage channels and flood-prone lowlands, making them particularly susceptible to inundation during extreme rainfall events. The settlements falling within the High Vulnerability category are presented in Table 9.

Table 9: Settlements Located in High Flood Vulnerability Zones

Settlement	Ward
Emmanuel Quarters	Oria
Ekuale Quarters	Emu
Odiotor	Oria
Oyebo Quarters	Emu
Ajouku Quarters	Oria
Agulere Quarters	Oria
Odumu Quarters	Oria
Erobobo	Illushi
Ifeanyi Quarters II	Oria
Osilika	Illushi
Alika	Illushi
Osualan Quarters	Oria
Owoli	Illushi
Ohikwakha	Oria
Ajobe	Illushi
Victor	Oria
Amalu Quarters	Oria
Okpatawo II	Illushi

The settlements listed in Table 9 are exposed to significant flood risk and may experience periodic inundation, disruption of transportation networks, damage to infrastructure, and loss of agricultural land during severe flood events. The spatial distribution of vulnerable settlements demonstrates that flood risk is not uniformly distributed across Esan South East LGA. The concentration of highly vulnerable settlements within Emu, Oria, and Illushi wards corresponds closely with the spatial distribution of the Very High Vulnerability zones identified in Figure 4. These areas coincide with low-lying terrain, extensive drainage networks, and zones of strong watershed influence. The findings suggest that future flood mitigation efforts should prioritize settlements located within the High and Very High Vulnerability classes. Structural measures such as drainage improvement, channel maintenance, and flood-control infrastructure, alongside non-structural approaches including land-use regulation, flood forecasting, and community awareness programmes, would contribute substantially to reducing flood-related losses within these communities.

3.6 Discussion of Results

The spatial pattern of flood vulnerability observed in Esan South East Local Government Area reflects the strong influence of landscape characteristics on the movement, accumulation, and concentration of surface runoff. The predominance of topographic and hydrological controls suggests that flooding within the area is largely a function of natural terrain configuration rather than isolated environmental conditions. Areas that combine low relief, limited drainage efficiency, and strong hydrological connectivity are inherently less capable of rapidly evacuating excess runoff, making them more vulnerable to inundation during intense or prolonged rainfall events.

The relatively high contribution of proximity to water bodies and drainage networks indicates that hydrological processes constitute the dominant mechanism driving flood vulnerability within the study area. Settlements and infrastructure located near rivers and drainage corridors are exposed not only to direct channel overflow but also to the cumulative effects of runoff generated from surrounding catchments. Such conditions increase the likelihood of recurrent flood events and amplify the potential magnitude of flood impacts. This relationship highlights the importance of preserving natural floodplains and restricting uncontrolled development along drainage corridors, which often serve as natural pathways for excess water during storm events.

The influence of elevation and slope demonstrates that terrain morphology plays an important role in regulating flood behaviour. Areas characterized by low elevations and gentle slopes tend to experience reduced runoff conveyance and prolonged water retention. These conditions favour the accumulation of floodwaters and increase the duration of inundation after rainfall events. Consequently, flood impacts within such environments may extend beyond immediate physical damage to include deterioration of road networks, disruption of transportation systems, reduced accessibility to services, and increased maintenance costs for public infrastructure.

The relatively balanced contribution of all conditioning factors suggests that flood vulnerability in Esan South East LGA cannot be attributed to a single environmental variable. Flood generation results from the interaction of multiple processes operating simultaneously at different spatial scales. Such complexity underscores the limitations of conventional single-factor assessments and justifies the application of integrated geospatial approaches capable of capturing the cumulative influence of several environmental variables. The findings therefore reinforce the value of multi-criteria decision analysis as a framework for understanding and managing flood-related hazards in complex landscapes.

The extent of land falling within moderate to very high vulnerability classes has significant implications for sustainable development within the Local Government Area. Areas identified as vulnerable are likely to experience increasing pressure as population growth and land development continue to expand into environmentally sensitive locations. Without adequate planning controls, future development may intensify exposure to flood hazards, increase economic losses, and place additional strain on local infrastructure. The results therefore highlight the need to integrate flood vulnerability information into land-use planning policies, development control regulations, and infrastructure siting decisions.

The vulnerability of several settlements further indicates that flooding represents not only an environmental challenge but also a socio-economic concern. Communities located within vulnerable zones may face repeated disruptions to livelihoods, particularly where agriculture constitutes a major economic activity. Flood-related damage to farmlands, transportation routes, and community facilities can reduce household income, constrain market access, and undermine local economic development. The concentration of vulnerable settlements within specific wards also suggests that flood impacts are unlikely to be evenly distributed across the LGA, thereby creating spatial inequalities in risk exposure and recovery capacity.

Findings from this study provide a basis for shifting flood management from a reactive approach centred on post-disaster response to a proactive strategy focused on risk reduction and resilience building. The flood vulnerability map offers a practical tool for identifying priority intervention areas, guiding infrastructure investments, and supporting the development of targeted adaptation measures. Such measures may include drainage improvement, watershed management, floodplain protection, and community-based preparedness programmes. Incorporating these interventions into local development planning would contribute to reducing future flood losses and enhancing the adaptive capacity of vulnerable communities.

The study also demonstrates that the integration of GIS, fuzzy logic, PCA, and Weighted Linear Combination techniques provides a scientifically robust framework for evaluating flood vulnerability in data-constrained environments. Beyond its application in Esan South East LGA, the approach offers a transferable methodology for supporting evidence-based flood management, environmental planning, and disaster risk reduction in other regions experiencing similar hydrological and topographic conditions.

4. Conclusion

This study assessed flood Vulnerability zones in Esan South East Local Government Area, Edo State, using Geographic Information System (GIS) techniques and a Multi-Criteria Decision Analysis (MCDA) framework. The integration of elevation, slope, proximity to drainage networks, proximity to water bodies, and watershed characteristics provided a comprehensive basis for evaluating the spatial variation of flood Vulnerability across the study area. The findings indicate that flood Vulnerability within the Local Government Area is controlled by the interaction of topographic and hydrological factors, which collectively influence the occurrence and distribution of flood-prone environments.

The application of fuzzy membership functions facilitated the standardization of heterogeneous datasets into a common analytical scale, while Principal Component Analysis (PCA) objectively established the relative importance of the selected flood-conditioning factors. The integration of the weighted factors through the Weighted Linear Combination (WLC) technique produced a spatially explicit flood Vulnerability model that successfully delineated areas according to their varying levels of Vulnerability. The resulting Vulnerability map revealed that while a considerable proportion of the study area falls within the very low and low Vulnerability classes, notable portions remain within the moderate, high, and very high Vulnerability categories, indicating the continued presence of significant flood-related challenges.

The analysis of settlement distribution further showed that several communities are located within zones characterized by elevated flood Vulnerability, thereby increasing their exposure to flood hazards and associated socio-economic impacts. Such exposure has implications for residential development, transportation infrastructure, agricultural activities, environmental management, and public safety. Persistent flooding in these areas may result in damage to infrastructure, disruption of economic activities, loss of agricultural productivity, and increased vulnerability of local populations.

The study demonstrates the applicability and effectiveness of integrating GIS, fuzzy logic, PCA, and WLC techniques for flood Vulnerability assessment. The adopted methodology provided a robust framework for identifying vulnerable locations and generating reliable spatial information for flood management. The flood Vulnerability map developed in this study serves as an important decision-support tool for land-use planning, infrastructure development, environmental management, disaster preparedness, and flood mitigation initiatives within Esan South East Local Government Area. The outcomes provide a scientific basis for strengthening flood resilience and promoting sustainable development within the study area. Furthermore, the methodological approach can be adapted and applied to other flood-prone regions facing similar environmental challenges.

Based on the findings of this study, it is recommended that future physical development projects, particularly residential, commercial, and public infrastructure developments, should be guided by the flood Vulnerability map to minimize exposure to flood hazards. Settlements and critical facilities located within high and very high Vulnerability zones should be prioritized for flood mitigation interventions, including improved drainage systems, flood control structures, and regular maintenance of existing waterways. Local and state government authorities should strengthen flood monitoring and early warning systems to enhance community preparedness and emergency response capabilities. Public awareness programmes should be implemented to educate residents on flood risks, preparedness measures, and appropriate responses during flood events. Agricultural activities within highly susceptible areas should incorporate climate-resilient and flood-adaptive practices to reduce potential losses. Future studies should also incorporate additional factors such as rainfall intensity, land use dynamics, soil characteristics, and climate change projections to further improve the accuracy and comprehensiveness of flood Vulnerability assessments.

References

[1] Gori, A., Blessing, R., Juan, A., Brody, S., and Bedient, P. (2019). Characterizing urbanization impacts on floodplain through integrated land use, hydrologic, and hydraulic modeling. *Journal of Hydrology, 568*, 82–95. https://doi.org/10.1016/j.jhydrol.2018.10.053

[2] Madsen, H., Lawrence, D., Lang, M., Martinkova, M., and Kjeldsen, T. R. (2014). Review of trend analysis and climate change projections of extreme precipitation and floods in Europe. *Journal of Hydrology, 519*, 3634–3650. https://doi.org/10.1016/j.jhydrol.2014.11.003

[3] Guha-Sapir, D., Hoyois, P., and Below, R. (2015). *Annual disaster statistical review 2015: The numbers and trends*. Centre for Research on the Epidemiology of Disasters (CRED).

[4] Montanari, A., and Koutsoyiannis, D. (2012). A blueprint for process-based modeling of uncertain hydrological systems. *Water Resources Research, 48*(9). https://doi.org/10.1029/2011WR011412

[5] Mandal, A., Stephenson, T. S., Brown, A. A., Campbell, J. D., and McKenzie, D. I. (2016). Rainfall-runoff simulations using the CARIWIG simple model for advection of storms and hurricanes and HEC-HMS: Implications of Hurricane Ivan over the Jamaica Hope River Watershed. *Natural Hazards, 83*, 1635–1659. https://doi.org/10.1007/s11069-016-2380-3

[6] Natural Resources Conservation Service. (2016). *Hydrologic analyses of post-wildfire conditions (Hydrology Technical Note No. 4)*. United States Department of Agriculture, Natural Resources Conservation Service.

[7] Lu, C., Zhou, J., He, Z., and Yuan, S. (2018). Evaluating typical flood risks in Yangtze River Economic Belt: Application of a flood risk mapping framework. *Natural Hazards, 94*, 1187–1210. https://doi.org/10.1007/s11069-018-3466-x

[8] Lee, Y. H., Kim, H. I., Han, K. Y., and Hong, W. H. (2020). Flood evacuation routes based on spatiotemporal inundation risk assessment. *Water, 12*(8), 2271. https://doi.org/10.3390/w12082271

[9] Li, C., Jiang, C., Chen, J., Lam, M. Y., Xia, J., and Ahmadian, R. (2025). An overview of flood evacuation planning: Models, methods, and future directions. *Journal of Hydrology, 656*, 133026. https://doi.org/10.1016/j.jhydrol.2025.133026

[10] Osman, S. A., and Das, J. (2023). GIS-based flood risk assessment using multi-criteria decision analysis of Shebelle River Basin in Southern Somalia. *SN Applied Sciences, 5*, 134. https://doi.org/10.1007/s42452-023-05360-5

[11] Mazarakis, V., Tsanakas, K., Greenbaum, N., et al. (2025). Flood-hazard assessment in the Messapios River catchment (Central Evia Island, Greece) by integrating GIS-based multi-criteria decision analysis and analytic hierarchy process. *Land, 14*(3), Article 658. https://doi.org/10.3390/land14030658

[12] Panagiotou, C. F. (2025). Copula-based assessment of flood susceptibility in the Island of Cyprus via stochastic multicriteria decision analysis. *Science of the Total Environment, 979*, 179469. https://doi.org/10.1016/j.scitotenv.2025.179469

[13] Moragues, A., Estrany, J., and Ruiz-Pérez, M. (2025). Assessment of social vulnerability to floods based on fuzzy logic in a Mediterranean dense urban area: Palma, Mallorca, Spain. *International Journal of Disaster Risk Reduction, 125*, 105594. https://doi.org/10.1016/j.ijdrr.2025.105594